

## Supporting Information

### **Unidirectional Supramolecular Self-Assembly inside Nanocorrals *via in situ* STM Nanoshaving**

Lander Verstraete, Jansie Smart, Brandon E. Hirsch,\* and Steven De Feyter\*

Department of Chemistry, Division of Molecular Imaging and Photonics, KU Leuven-University  
of Leuven, Celestijnenlaan 200F, B-3001 Leuven, Belgium.

#### **Contents**

1.	Cyclic Voltammetry.....	S2
2.	Corral Apex Angle.....	S2
3.	Nanoshaving Tip Speed.....	S7
4.	Nanoshaving Line Spacing.....	S8
5.	Nanoshaving Set Point Current.....	S11
6.	Nanoshaving Voltage Bias.....	S12
7.	Stability of Assemblies against Nanoshaving Conditions.....	S15
8.	Stability of Assemblies against Imaging Conditions.....	S16

## 1. Cyclic Voltammetry

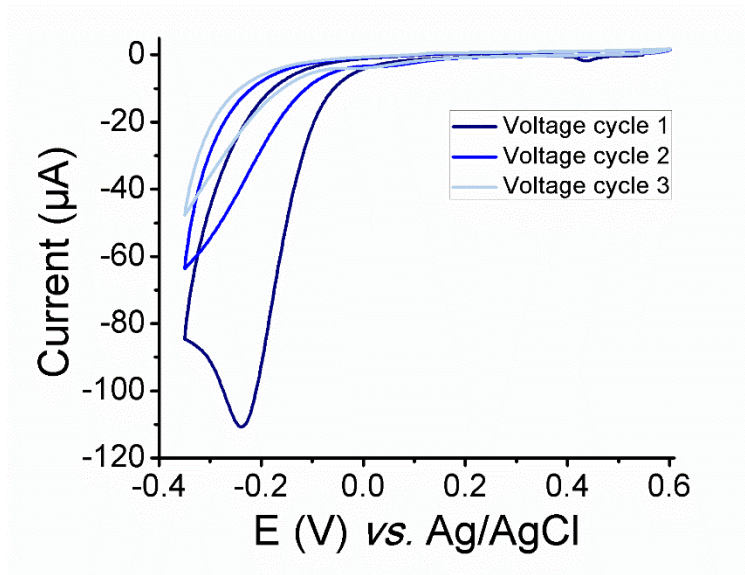


**Figure S1.** Cyclic voltammogram of 2 mM 3,5-bis-*tert*-butylbenzenediazonium in 50 mM HCl, using HOPG as a working electrode. Scan rate: 0.1 V/s.

## 2. Corral Apex Angle

Three individual experiments were conducted, each investigating four discrete apex angles. Other shaving parameters are  $I_t = 200$  pA,  $V_{tip} = 0.001$  V,  $v_{tip} = 0.4$   $\mu\text{m/s}$  and *line spacing* = 0.6 nm. Nanoshaving was performed in a 4 x 4 matrix format and the apex angles were varied randomly within the matrix. Two different matrix layouts, shown in Figure S2, were used alternatingly. The corral area for each apex angle is shown in Figure S3. 158 and 180, and 154 nanocorrals were analyzed for experiment 1, 2, and 3, respectively.

Each apex angle was measured from the raw STM images. To obtain the most accurate apex angle values only the top third of the triangle was considered, as illustrated in Figure S4. Angles that were much larger or smaller than the intended shape were reassigned to the most applicable group in order to avoid overlap between different groups. The distribution of apex angles for each of the four groups is shown in Figure S5.

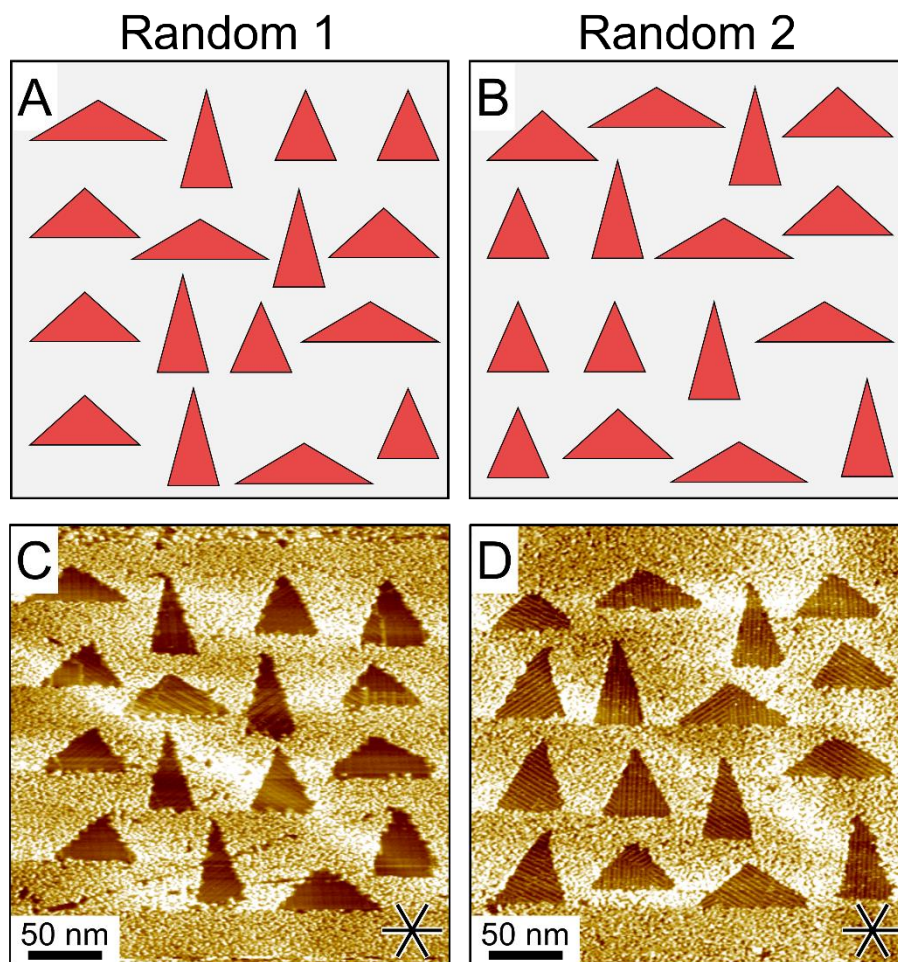


**Figure S2.** (a-b) Schematic layout of the two random matrix designs that were used to investigate the effects of corral apex angle. (c-d) Corresponding STM images. Imaging parameters:  $I_t = 200$  pA,  $V_{sample} = -0.8$  V.

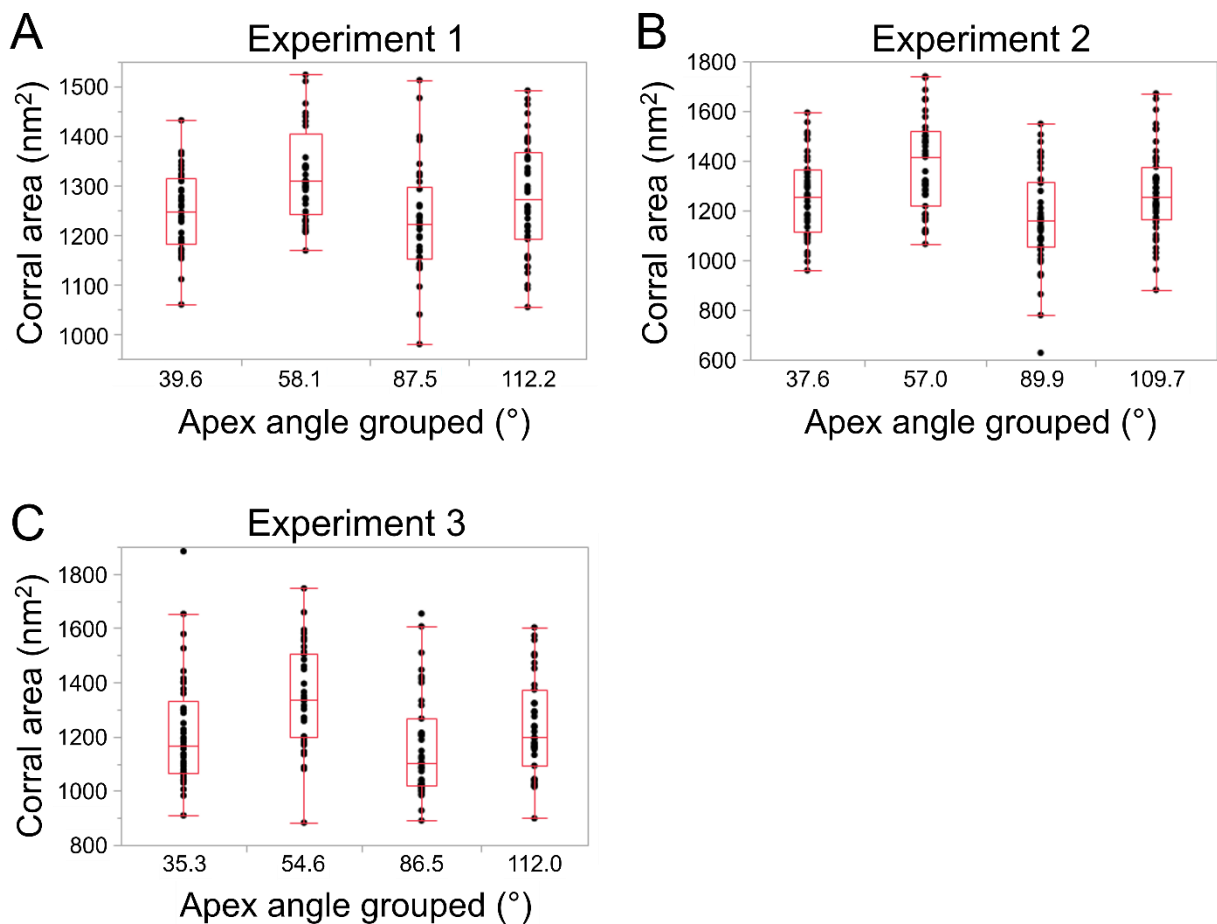


**Figure S3.** Corral area as a function of triangle apex angle for experiment 1,2, and 3, respectively. The grouped angles are represented by the average angle value. Box plots are overlaid in red.

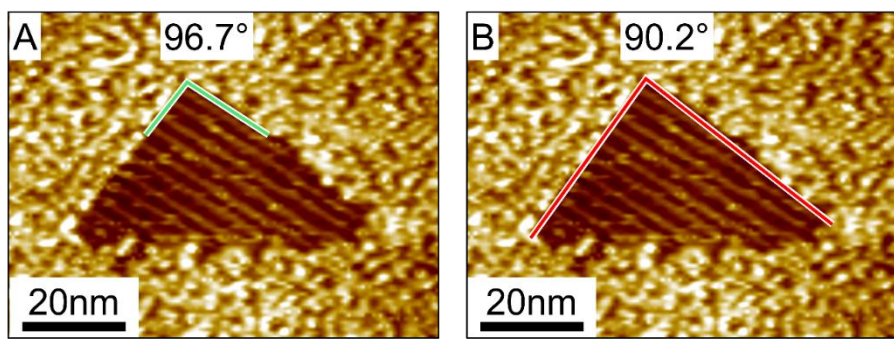


**Figure S4.** (a) Only the top third of the total corral is considered for measuring the apex angle. (b) The total corral is considered for measuring the apex angle. The method in (a) is believed to give more accurate measurements and was used for analyzing the data in this work. Imaging parameters:  $I_t = 200$  pA,  $V_{sample} = -0.8$  V.

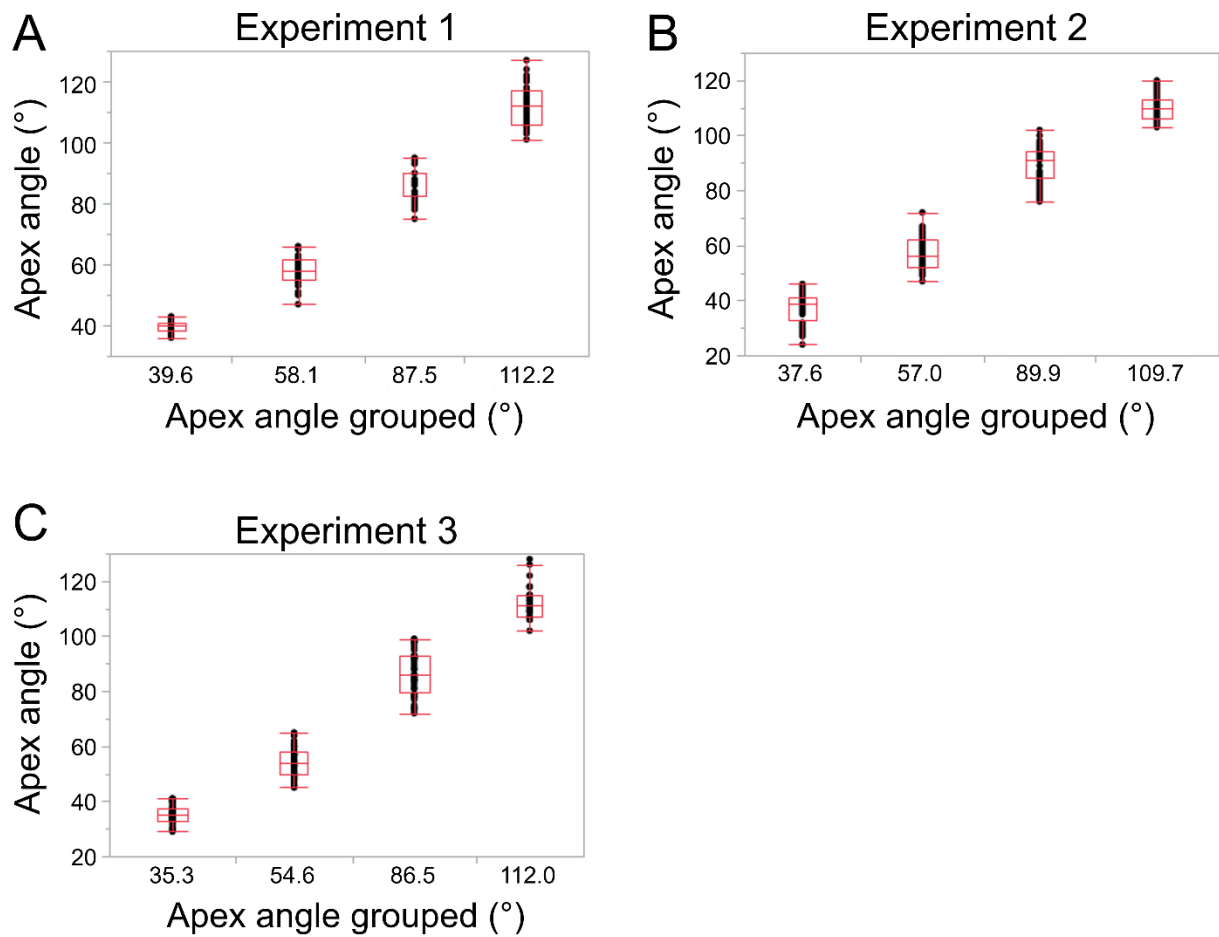


**Figure S5.** Apex angle grouping for experiment 1,2, and 3, respectively. The groups are designated by the average apex angle value of that group. Box plots are overlaid in red.

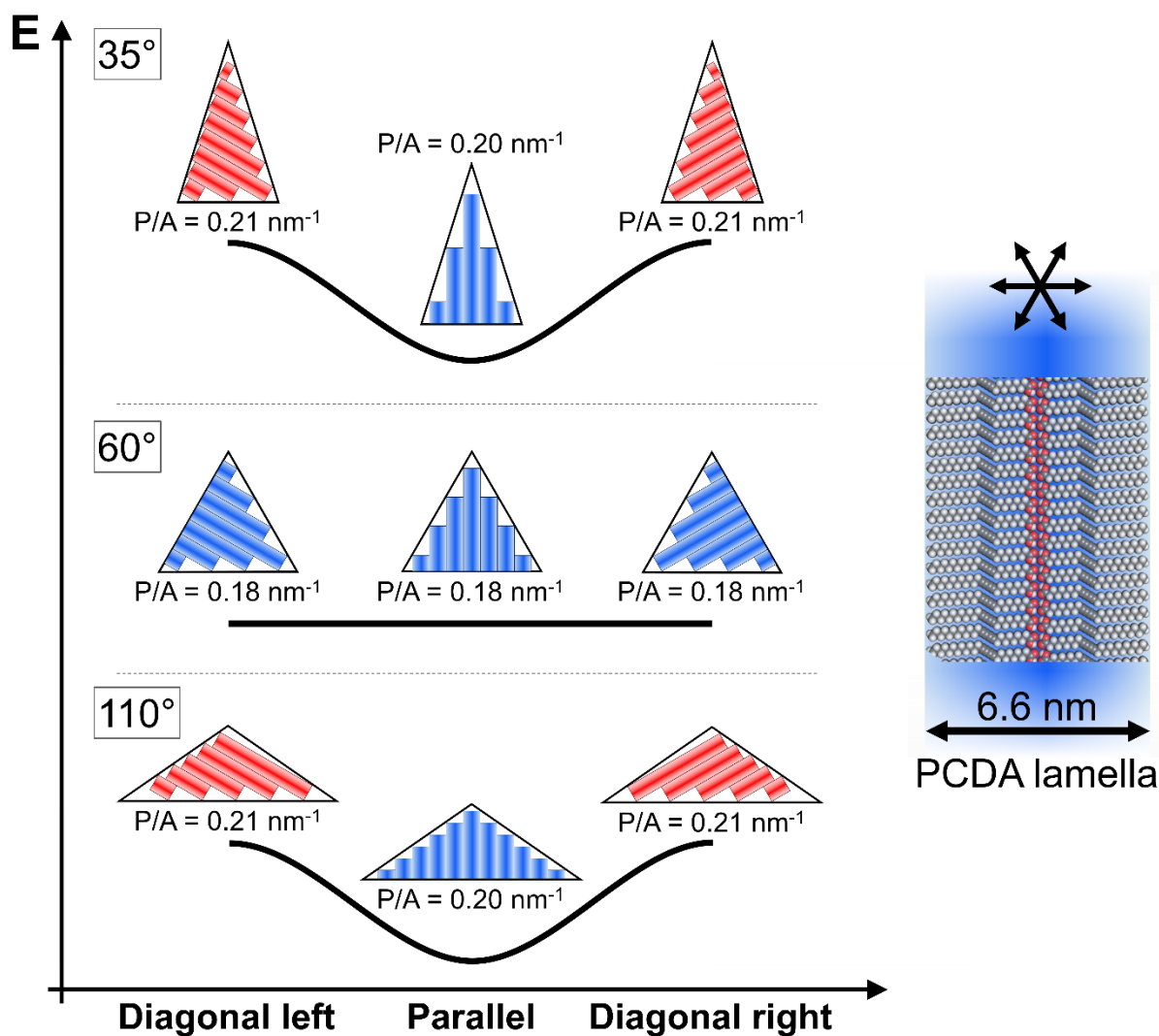


**Figure S6.** Schematic showing how lateral constraints impact different PCDA assembly orientations for acute, equilateral and obtuse triangles. For simplicity, PCDA lamellae are represented as columns of PCDA dimers (right). The nanocorrals were filled with as much PCDA assembly as geometrically allowed. Using estimated values of corral area ( $1250 \text{ nm}^2$ ) and lamella width (6.6 nm), the assembly perimeter to area ratio (P/A) was determined. The relative energy axis is based upon the assumption that PCDA assemblies get more stable as P/A decreases. Inside acute and obtuse triangles, P/A is slightly higher for diagonal assemblies than for parallel assemblies. As a result, diagonal assemblies are expected to be energetically unfavorable compared to their parallel analogue. On the other hand, inside equilateral triangles all assembly orientations have the same P/A ratio and are thus energetically equal. Overall, it can thus be understood that lateral constraints force PCDA molecules in a parallel orientation inside corrals that do not match the threefold rotational symmetry of the substrate.

### 3. Nanoshaving Tip Speed

Three individual experiments were carried out, each investigating six different shaving tip speed values. Other shaving parameters were kept constant:  $I_t = 200$  pA,  $V_{tip} = 0.001$  V, and *line spacing* = 0.6 nm. Nanoshaving was performed in a 4 x 4 matrix format with 16 identical equilateral triangles. The tip speed was kept constant within a matrix, but varied randomly from one matrix to another. Tip speed values were repeated only when a complete sequence of six values was finished. An STM image of 4 x 4 corrals created with  $v_{tip} = 0.12$   $\mu\text{m/s}$  is shown in Figure S7. In total 378, 462, and 367 corrals were analyzed for the three experiments, respectively. It is important to point out that, due to the design of the PicoLITH software package for nanoshaving, there is no linear correlation between the nanoshaving tip speed and the total shaving time. The nonlinearity between shaving tip speed and the shaving time is illustrated in Figure S8.

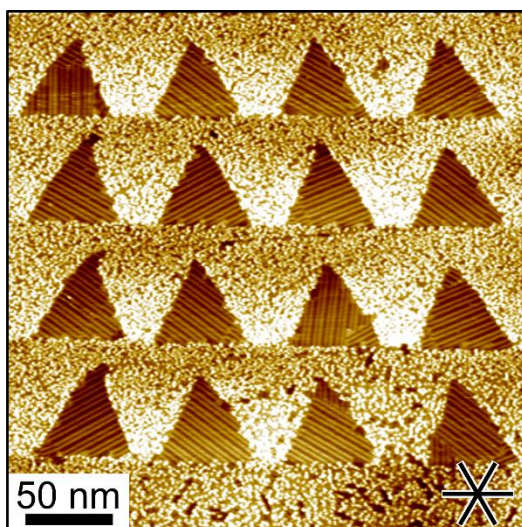


**Figure S7.** STM image displaying 16 equilateral triangles shaved at a tip speed of 0.12  $\mu\text{m/s}$ . Imaging parameters:  $I_t = 60$  pA,  $V_{sample} = -0.8$  V.

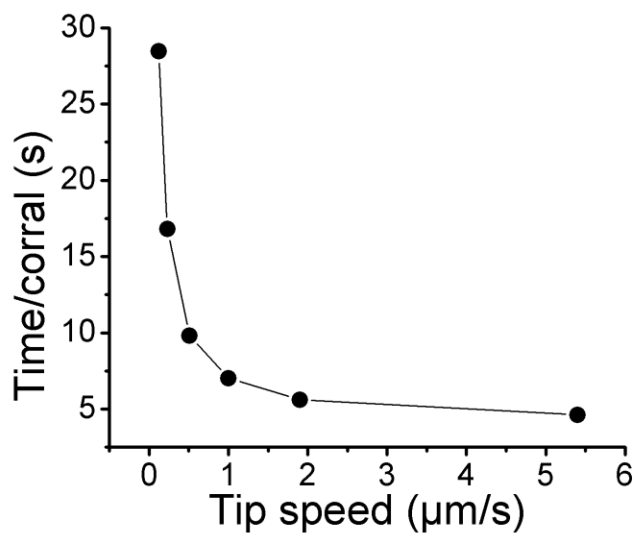


**Figure S8.** Graph illustrating the nonlinearity between the total time needed to nanoshave a corral and the tip speed during shaving.

#### 4. Nanoshaving Line Spacing

The effect of nanoshaving line spacing on PCDA self-assembly was examined for two individual experiments, each investigating four line spacing values. Other shaving parameters were kept constant:  $I_t = 200$  pA,  $V_{tip} = 0.001$  V, and  $v_{tip} = 1$   $\mu\text{m/s}$ . Nanoshaving was performed in a 4 x 4 matrix format with 16 equilateral triangles. The line spacing values were varied randomly within a matrix. Two random matrix layouts were used alternately as illustrated in Figure S9. Upon increasing the line spacing, a point will be reached where no longer all grafted molecules are removed, as illustrated for square nanocorrals in Figure S10. In the range of line spacings tested here (0.6 nm to 2.4 nm), incomplete nanoshaving is observed only occasionally as shown in Figure S11. All corrals with incomplete shaving were excluded from further analysis. 277 and 325 corrals were analyzed for experiment 1 and 2, respectively.

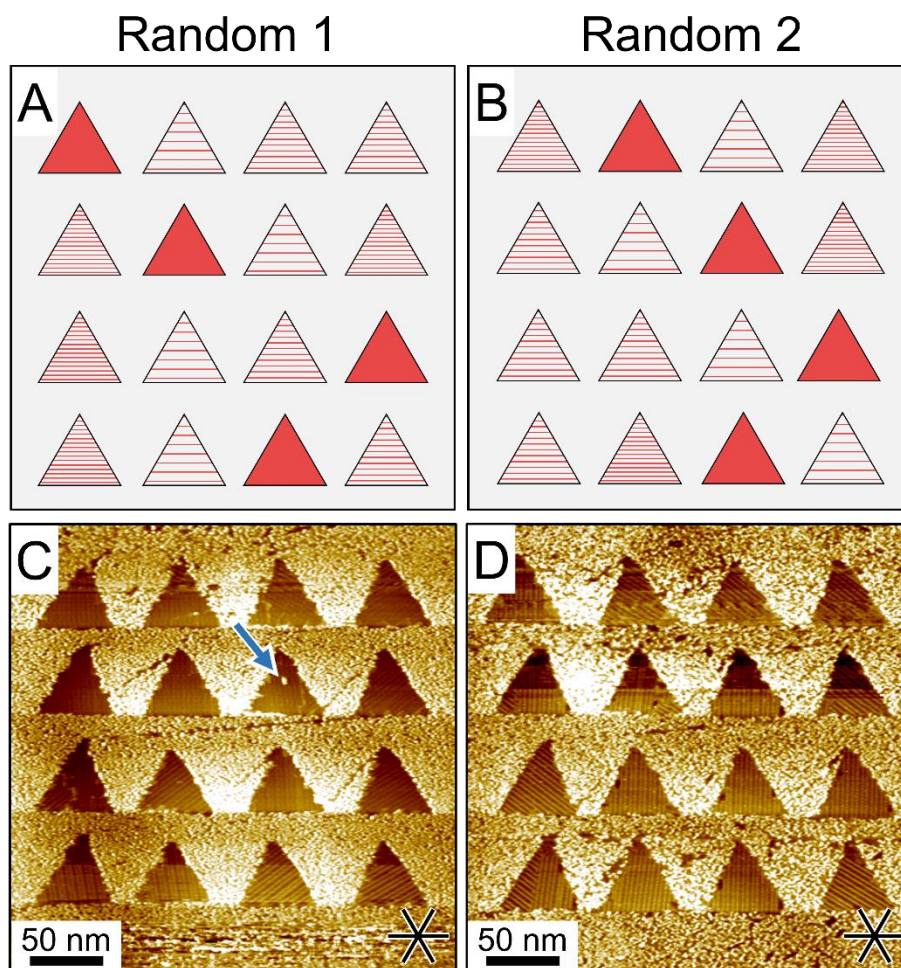


**Figure S9.** (a-b) Schematic layout of the two random matrix designs that were used to examine the effects of nanoshaving line spacing. (c-d) Corresponding STM images. The blue arrow in (c) points at a remaining grafted aryl. Imaging parameters:  $I_t = 200$  pA,  $V_{sample} = -0.8$  V.

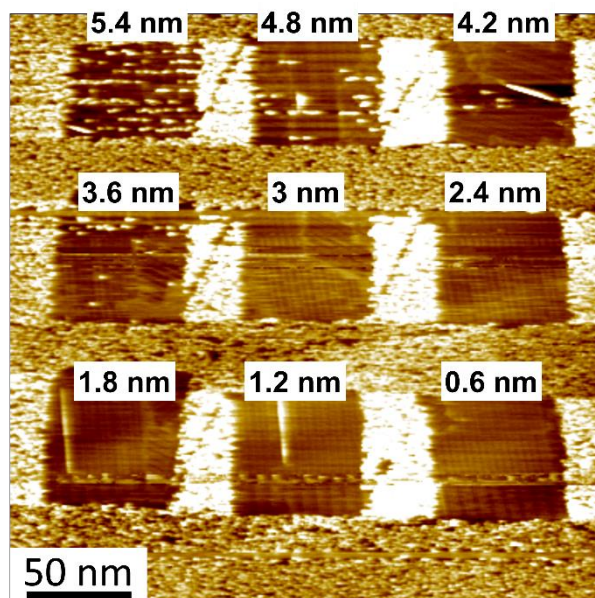


**Figure S10.** Nanoshaving of square nanocorrals at different line spacing values. In this image incomplete nanoshaving is evident starting from a spacing  $\geq 3.6$  nm. Imaging conditions:  $I_t = 60$  pA,  $V_{sample} = -0.8$  V.

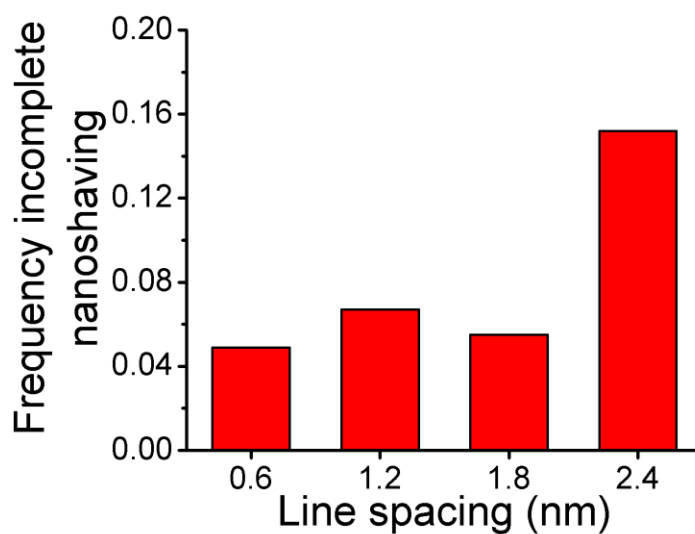


**Figure S11.** Frequency of incomplete nanoshaving as a function of line spacing. The data were acquired by combining the two individual experiments.

## 5. Nanoshaving Set Point Current

The impact of set point current during nanoshaving on PCDA self-assembly was investigated by nanoshaving with six discrete current values. All other shaving parameters were fixed at  $V_{tip} = 0.01$  V,  $v_{tip} = 0.4$   $\mu\text{m/s}$ , and  $line\ spacing = 0.6$  nm. Equilateral triangular corrals were created in a 4 x 4 matrix format. The current values were kept constant within one matrix, but were varied from matrix to matrix. Current values were repeated only when a complete sequence of six values was finished. An STM image of 4 x 4 corrals shaven with  $I_t = 75$  pA is shown in Figure S12. Nanoshaving was not always complete as shown in Figure S13. Two individual experiments were performed for which 446 and 553 corrals were analyzed, respectively.

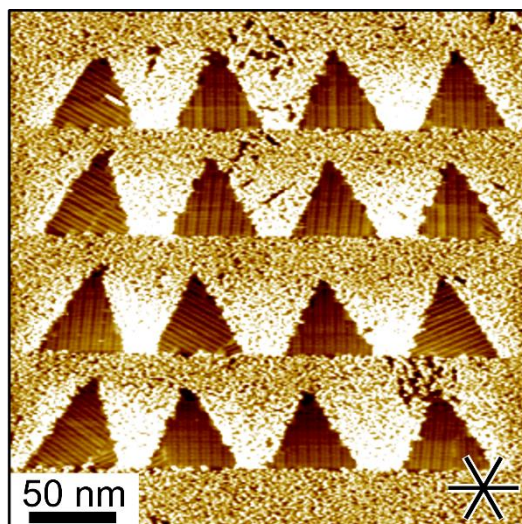


**Figure S12.** STM image of 4 x 4 equilateral triangles created with a nanoshaving set point current of 75 pA. Imaging parameters:  $I_t = 200$  pA,  $V_{sample} = -0.8$  V.

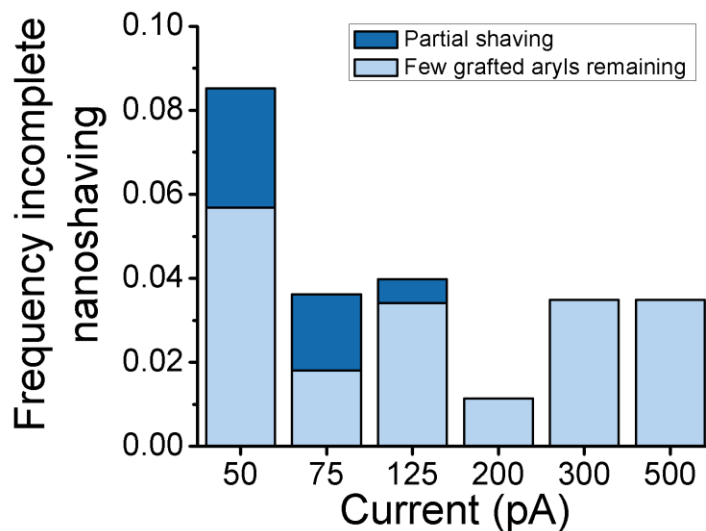


**Figure S13.** Frequency of incomplete nanoshaving for different set point currents. A distinction was made between partial shaving and a few grafted aryls remaining. Exemplary STM images are shown in Figure S23. The data were acquired by combining two individual experiments.

## 7. Nanoshaving Voltage Bias

The impact of the magnitude of applied tip bias during nanoshaving on PCDA self-assembly was investigated by nanoshaving equilateral triangular corrals with four discrete tip bias values (positive tip bias & negative sample bias). All other shaving parameters were fixed at  $I_t = 200$  pA,  $v_{tip} = 0.4$   $\mu\text{m/s}$ , and *line spacing* = 0.6 nm. Two different experimental matrix designs referred to as Random 1 and Random 2 were used alternately (Figure S14a,b). Representative STM images of matrices obtained with both designs are shown in Figure S14c,d. No corral was created in the upper left corner in Figure S14d due to too mild shaving conditions. The frequency of incomplete nanoshaving as a function of applied bias is shown in Figure S15. Two independent experiments were performed for which PCDA self-assembly was analyzed inside 572 and 326 corrals, respectively.

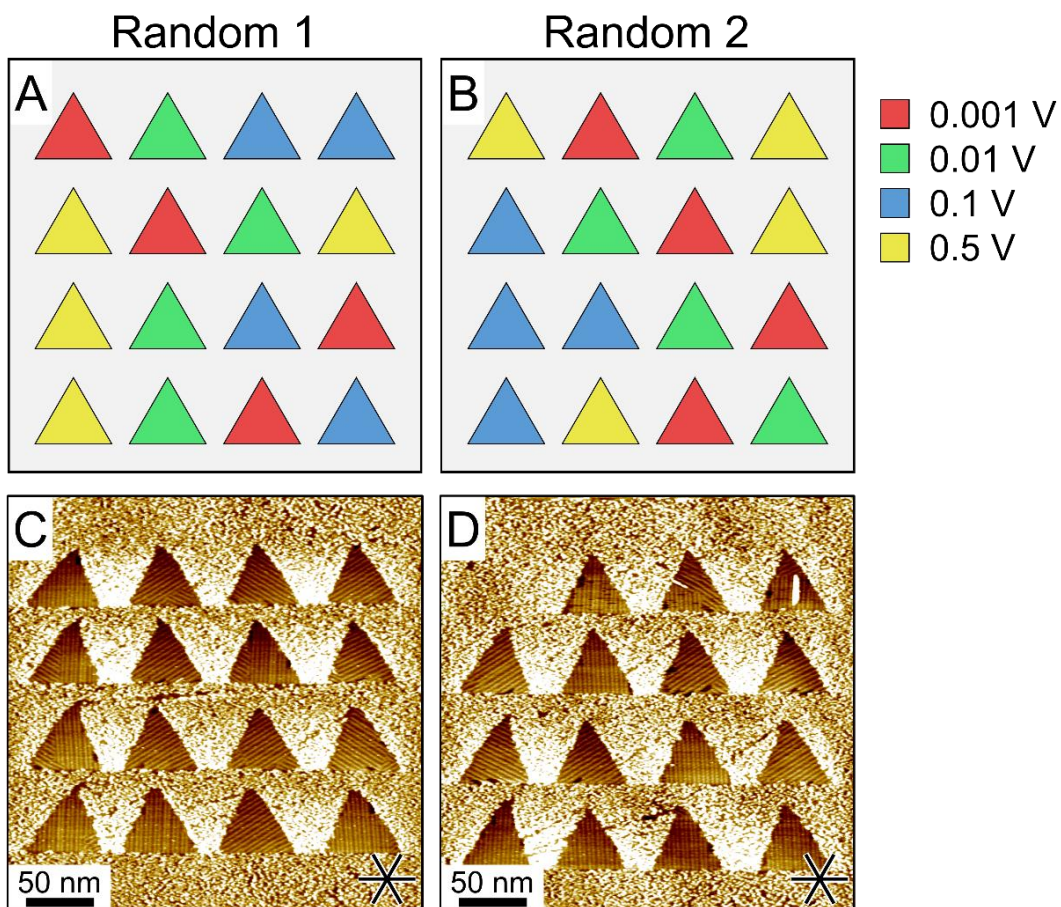


**Figure S14.** (a-b) Experimental layout of the Random 1 and Random 2 designs that were used alternately for nanoshaving at different tip biases. The color code represents the tip bias during nanoshaving. (c-d) STM images showing a 4 x 4 matrix of equilateral triangles that were created according to the Random 1 and Random 2 design for nanoshaving, respectively. Imaging parameters:  $I_t = 200$  pA,  $V_{sample} = -0.8$  V.

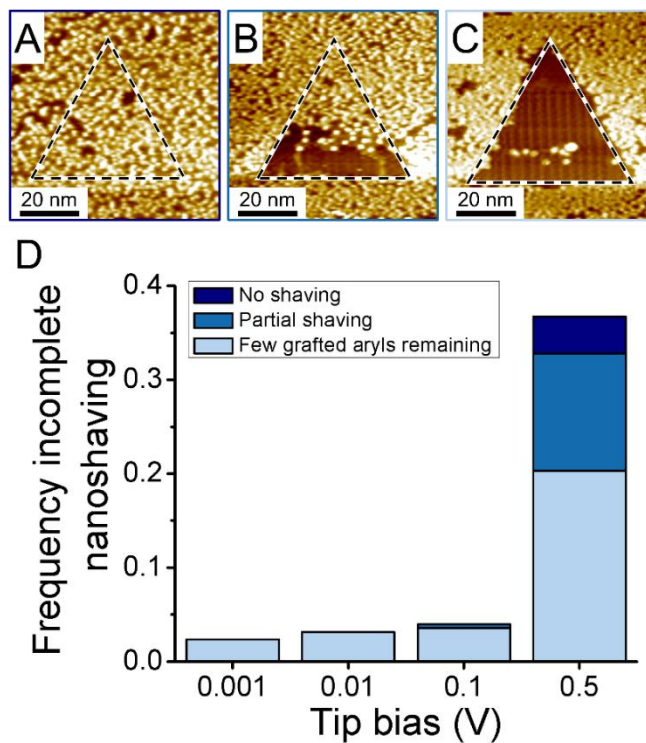


**Figure S15.** (a-c) STM images showing examples of incomplete nanoshaving. A distinction was made between (a) no shaving, (b) partial shaving, and (c) a few grafted molecules remaining. Imaging conditions:  $I_t = 60$  pA and  $V_{sample} = -0.8$  V. (d) Frequency of incomplete nanoshaving as a function of applied tip bias. The data were obtained by combining two individual experiments.

## 9. Stability of Assemblies against Nanoshaving Conditions

A

N° rotational domains	Assembly orientation(s)	Relative occurrence
Single PCDA domain	Assembly along 1 <sup>st</sup> shaving direction	0.49
	Assembly along 2 <sup>nd</sup> shaving direction	0.16
	Assembly along 3 <sup>rd</sup> direction	0.16
Multiple PCDA domains	Matching shaving directions	0.16
	Not matching shaving directions	0.03

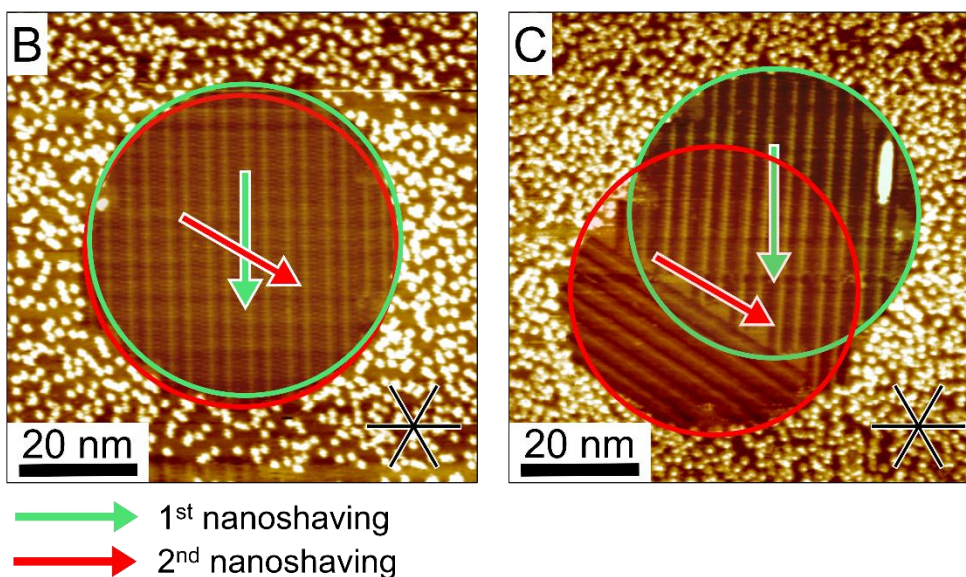


**Figure S16.** Stability of PCDA assemblies against nanoshaving conditions. Immediately after the first nanoshaving event, nanoshaving was repeated along a different, but equivalent, substrate symmetry direction. Importantly, to avoid large spatial offsets between the two nanoshaving events, no imaging was performed in between the two nanoshaving events. As such the orientation of self-assembly after the first nanoshaving event is not known *per se*. The relative occurrence of assembly orientations with respect to the shaving directions is shown in (a). In the case of a single PCDA domain, the majority of domains was oriented along the initial shaving direction as illustrated in (b). Occasionally, multiple rotational domains were observed when the spatial offset between the two nanoshaving events was too large. In the case of multiple rotational domains, they generally coincided with the two nanoshaving directions, as illustrated in (c). Overall, no correlation between the assembly and second nanoshaving direction was observed. In total, 37 corrals were investigated. The arrows in (b) and (c) represent the slow nanoshaving directions. Nanoshaving conditions:  $I_t = 200$  pA,  $V_{tip} = 0.001$  V,  $v_{tip} = 0.4$   $\mu\text{m/s}$ , and *line spacing* = 0.6 nm. Imaging conditions:  $I_t = 60$  pA,  $V_{sample} = -0.8$  V.

## 10. Stability of Assemblies against Imaging Conditions

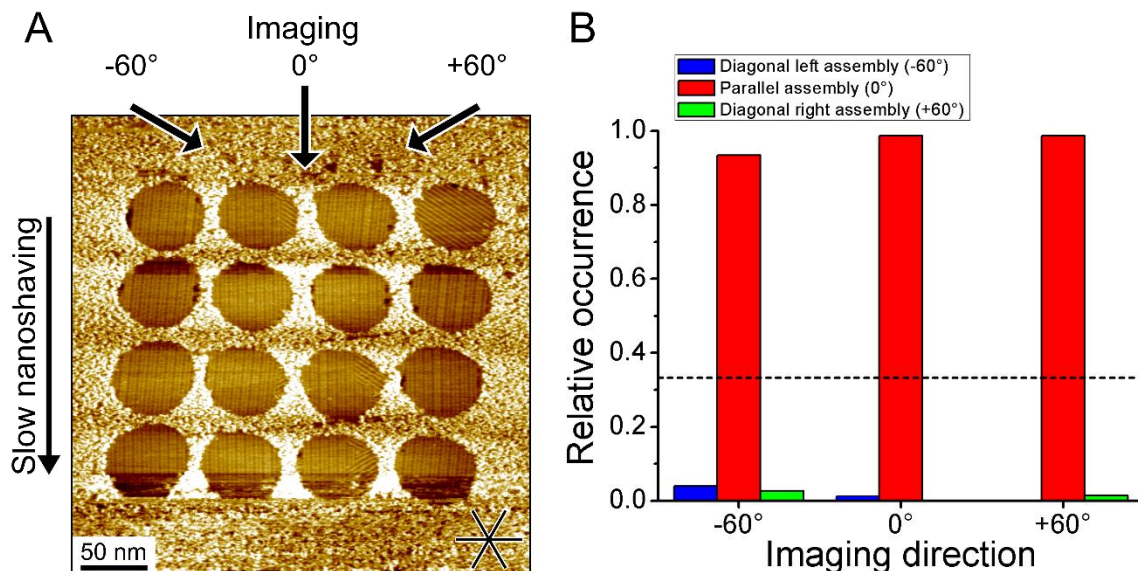


**Figure S17.** Stability of PCDA assemblies against imaging conditions ( $I_t = 60$  pA,  $V_{sample} = -0.8$  V). First, a matrix of 4 x 4 identical circular nanocorrals was created with the following nanoshaving conditions:  $I_t = 200$  pA,  $V_{tip} = 0.001$  V,  $v_{tip} = 2$   $\mu\text{m/s}$ , and *line spacing* = 0.6 nm. Next, imaging was performed under an angle of  $-60^\circ$ ,  $0^\circ$ , or  $60^\circ$  with respect to the slow nanoshaving direction, as illustrated in (a). The relative occurrence of different PCDA assembly orientations as a function of the imaging direction is shown in (b). The dashed line represents the theoretical, unconstrained self-assembly outcome. The obtained statistics revealed no apparent correlation between the assembly orientation and the imaging direction (Pearson correlation test,  $p = 0.231$ ). Rather, PCDA assemblies that are parallel to the slow nanoshaving direction (*i.e.* parallel assemblies) were strongly preferred, irrespective of the imaging direction. It can thus be concluded that the assemblies obtain their orientation during nanoshaving, and that subsequent imaging scans have no profound effects. 227 nanocorrals were investigated in total.